

See discussions, stats, and author profiles for this publication at: <https://www.researchgate.net/publication/6949951>

Reactivity of Oxide Precursor States on Ru(0001)

ARTICLE in THE JOURNAL OF PHYSICAL CHEMISTRY B · JULY 2006

Impact Factor: 3.3 · DOI: 10.1021/jp061937a · Source: PubMed

CITATIONS

3

READS

10

3 AUTHORS, INCLUDING:



Wolfgang Christen

Humboldt-Universität zu Berlin

31 PUBLICATIONS 398 CITATIONS

SEE PROFILE



Horst Niehus

Humboldt-Universität zu Berlin

165 PUBLICATIONS 4,465 CITATIONS

SEE PROFILE

Reactivity of Oxide Precursor States on Ru(0001)

Raoul Blume,^{*,†} Wolfgang Christen,[†] and Horst Niehus[‡]

*Institut für Chemie, Humboldt-Universität zu Berlin, Brook-Taylor-Strasse 2, 12489 Berlin, Germany, and
Institut für Physik, Humboldt-Universität zu Berlin, Newtonstrasse 15, 12489 Berlin, Germany*

Received: March 29, 2006; In Final Form: April 27, 2006

Smooth and defect-rich Ru(0001) surfaces prepared under ultrahigh-vacuum (UHV) conditions have been loaded with oxygen under high-pressure ($p \leq 1$ bar) and low-temperature ($T < 550$ K) conditions. On these surfaces the CO oxidation reaction has been investigated by means of thermal desorption spectroscopy (TDS), ultraviolet photoelectron spectroscopy (UPS) and reactive molecular beam scattering (RMBS). Both surfaces are oxide-free and exhibit a high reactivity. The maximum CO/CO₂ conversion probability observed for a defect-rich Ru(0001) surface amounts to 6×10^{-3} and is comparable to that of a surface covered with rutile RuO₂(110) domains. RMBS experiments led to the identification of three different reaction channels. The first and second channel is related to CO adsorbing at oxygen-free defect sites and follow the Langmuir–Hinshelwood mechanism. Whereas the first reaction channel is already observed at room temperature, the second is thermally activated, contributing to the CO₂ yield only for reaction temperatures above 400 K. The third channel is due to the recombination of CO molecules with oxygen atoms located in smooth areas of the surface undisturbed by defects. This reaction channel is thermally activated as well.

1. Introduction

The development and improvement of chemical process technologies is closely related to the quality of the employed catalysts. Transition metals are well-known for their chemical activity and are widely used to promote a large variety of catalytic reactions. Ruthenium represents a very versatile element both in homogeneous and in heterogeneous catalysis, e.g., in hydrogenation and hydroxylation reactions,^{1,2} in ring opening metathesis polymerization³ and also in fuel cells as anode material.⁴

In practical applications such as the purification of automotive exhausts, the oxidation process of carbon monoxide is highly relevant. In general, this reaction requires temperatures significantly above room temperature and pressures beyond UHV conditions, making it a difficult task to characterize the elemental processes involved in the reaction. One approach toward a better understanding of the basic mechanisms underlying this oxidation reaction is the preparation of single-crystal Ru samples under UHV conditions. Most transition metals show a high activity in the CO/CO₂ conversion under both UHV and high-pressure conditions, as long as the amounts of oxygen and CO adsorbed on the sample surface are in equilibrium.⁵ Ruthenium is found to be highly reactive only under high-temperature and -pressure conditions^{6,7} whereas under UHV conditions virtually no CO oxidation can be observed.⁸ Recently, this so-called “pressure gap” has been narrowed by applying moderate pressures up to 10^{-3} mbar at temperatures higher than 600 K, resulting in the growth of oxide domains.^{6,9} While for a chemisorbed oxygen layer the reaction probability for the CO/CO₂ conversion does not exceed 10^{-4} , on a partially oxidized surface prepared under these high-temperature (HT) conditions the reaction probability increases up to 10^{-2} .^{6,10} This strong enhancement of the reaction

yield was attributed to coordinatively unsaturated ruthenium atoms in the topmost layer of the RuO₂ domains where CO and oxygen can easily adsorb and successively react to CO₂.¹¹

The morphology of a surface^{12,13} also plays an important role for catalytic processes. In the case of ruthenium it was found after preparation under high-temperature and -pressure conditions that the areas between oxide domains are heavily loaded with oxygen without exhibiting the typical indications of bulk oxide formation.^{14,15} These areas may contribute to the increased reaction yield observed for the CO oxidation process. However, such intermediate or precursor states to the actual oxide formation are difficult to investigate. Due to the pronounced oxide domain growth in the HT regime, the preparation window in which such states can be generated without bulk oxide formation is extremely small.

Applying high oxygen pressures at comparably low temperatures (below 550 K, hence LT preparation),¹⁶ we were able to create these oxide precursor states, also labeled “subsurface oxygen” or “surface oxide”, on the Ru(0001) surface up to oxygen contents equivalent to ≈ 3 monolayers (ML). This report examines the reactivity of these states toward the CO/CO₂ conversion by means of thermal desorption spectroscopy (TDS) and ultraviolet photoelectron spectroscopy (UPS). To assess the surface sites responsible for the reaction, we intentionally created defects on the surface and studied their influence on reactivity. For further insights, we applied reactive molecular beam scattering (RMBS) to monitor the temporal behavior of the CO₂ reaction yield and to study the influence of morphology on the reaction pathways.

2. Experimental Section

The experiments were conducted in a UHV chamber at a base pressure of less than 2×10^{-10} mbar. The vacuum system is equipped with standard facilities for sample cleaning and sample characterization (quadrupole mass spectrometer (QMS), low-energy electron diffraction (LEED)/Auger electron spectroscopy

* Corresponding author. E-mail: raoul.blume@physik.hu-berlin.de.
Phone: ++4930-2093-7720.

[†] Institut für Chemie.

[‡] Institut für Physik.

(AES), TDS, and UPS (21.2 eV)). It has been designed to allow high oxygen exposures at partial pressures up to 1 bar and fast oxygen pumping reaching UHV conditions ($p < 5 \times 10^{-9}$ mbar) within 15 min.¹⁶ The UHV chamber is connected to a molecular beam apparatus providing helium atom scattering (HAS) and the surface interaction of reactive gases such as CO with well-defined translational energy. Particles scattered off the target surface have been probed by a QMS in specular direction ($\Theta_{\text{In}} + \Theta_{\text{Out}} = 45^\circ$) with an acceptance angle of $\approx 15^\circ$.

The Ru(0001) crystal has been cleaned by several cycles of Ar⁺ sputtering (2 kV, 3–10 μA for 10 min) and subsequent annealing to 1550 K as well as baking at 1100 K in an oxygen atmosphere of 10^{-7} mbar for 10 min.^{8,17} After a final heating of the sample to 1550 K, no residual oxygen traces could be detected by either TDS or UPS and AES. Nevertheless, to exclude a long-term degradation of the subsurface region by a possible oxygen accumulation in deeper bulk regions, every new oxidation procedure of Ru(0001) was preceded by several sputtering and annealing cycles.

The incorporation of oxygen into the topmost layers of the ruthenium surface has been achieved by exposing the cleaned sample to high-purity molecular oxygen (Messer Griesheim, 99.997% purity) at constant partial pressure in the range of 10^{-9} mbar to 1 bar. The oxygen exposure was started only after reaching a fixed, stabilized sample preparation temperature, T_{P} , which was monitored by a K-type thermocouple spot-welded to the backside of the crystal. The partial pressure was recorded using IKR060 and TPR018 pressure gauges (Balzers) for pressures below and above 10^{-3} mbar, respectively. Thermal desorption spectra were taken with a constant heating rate of 4 K/s realized by resistive heating of the sample. The oxygen content of the Ru sample was determined by numerically integrating the TD spectra of the desorbing oxygen. TD data were calibrated with the LEED image of a saturated adsorbed oxygen layer ($\Theta = 1$) which forms a $(1 \times 1)\text{-O}$ superstructure.⁶ Thus the oxygen coverage is expressed in terms of monolayers with $1 \text{ ML} = 1.58 \times 10^{15} \text{ molecules/cm}^2$ and an estimated accuracy of $\pm 0.2 \text{ ML}$.

Additional surface defects can be created on purpose by exposing the clean, annealed surface to a weak flux of low-energy Ar⁺ ions (500 eV, 0.7 μA). This soft sputtering procedure is applied only after the preceding He atom scattering revealed a minimum surface roughness. Details of the HAS-based determination of the surface roughness are discussed elsewhere.¹⁸ In short, one obtains a roughness ratio defined by $\rho = (I_{\text{smooth}} - I_{\text{rough}})/I_{\text{smooth}}$, from the scattered He intensities of the smooth (I_{smooth}) and the rough surface (I_{rough}) measured while the sample is heated from room temperature to 1550 K. The maximum mean surface roughness achievable for Ru(0001) is $\rho = 0.4$.

The supersonic beam of CO was produced by adiabatic expansion of pure carbon monoxide (Messer Griesheim, 99.997% purity) at room temperature and a stagnation pressure of 3 bar through a 20 μm diameter nozzle into a vacuum chamber at working pressures below 10^{-3} mbar. The expanding jet is collimated by a skimmer, resulting in a beam diameter at the sample surface of $\approx 7 \text{ mm}$. This beam provides a constant flux of $\approx 3 \times 10^{14} \text{ molecules/(cm}^2 \text{ s)}$ with a kinetic energy of $\approx 90 \text{ meV/molecule}$.¹⁹

3. Results

A. CO₂ Reaction Yields and the TDS β State. Applying TDS, characteristic features of oxide precursor states on Ru(0001) prepared at low-temperature conditions (LT; $T_{\text{P}} < 550$

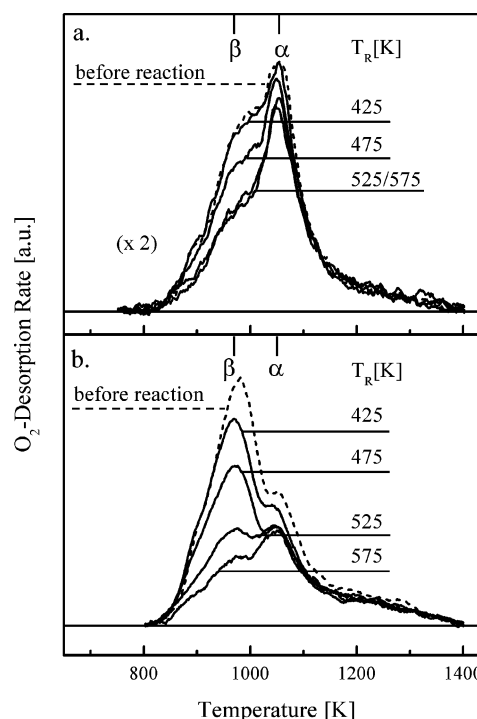


Figure 1. Comparison of TD spectra of O₂ before (dashed) and after the reaction (solid) with 1000 langmuirs of CO at reaction temperatures $425 \text{ K} < T_{\text{R}} < 575 \text{ K}$ of an oxidized smooth (a) and a defect-rich (b) Ru(0001) surface ($\rho = 0.4$). The surfaces were oxidized with 10^{11} langmuirs of O₂ at $T_{\text{P}} = 475 \text{ K}$.

K) are three distinct desorption maxima of molecular oxygen.¹⁶ The most prominent peaks centered at ≈ 1040 and $\approx 970 \text{ K}$ (named α and β , respectively) mirror the incorporation of subsurface oxygen, which depends on the defect density of the surface.¹⁸ The third peak, desorbing over a broad temperature range above 1100 K is related to the desorption of a full oxygen layer chemisorbed on top of the first ruthenium layer and is used for calibration of the oxygen content. TD spectra representing the desorption of molecular oxygen from a nearly defect-free and a defect-rich Ru surface that have been exposed to 10^{11} langmuirs of oxygen at a preparation temperature $T_{\text{P}} = 475 \text{ K}$ are shown in Figure 1a,b (dashed curves). Figure 1a compares the TD spectrum of oxygen from the nearly defect-free Ru surface with a total of $\approx 2.7 \text{ ML}$ oxygen (dashed curve) to TD spectra of similarly prepared surfaces after the oxidation of 1000 langmuirs of CO at different T_{R} . The peak intensities of these TD spectra depend on the reaction temperature T_{R} . With increasing T_{R} the intensity of desorption peak β is decreasing whereas the intensity of peak α remains nearly unaffected. At higher reaction temperatures (525 and 575 K), the resulting TD spectra become indistinguishable within our experimental error. Apparently, the intensity of peak β does not decrease any further at higher T_{R} . For comparison, Figure 1b shows TD spectra of the defect-rich surface ($\rho = 0.4$) with the same preparation. Due to the larger defect density,¹⁸ a considerably higher amount of oxygen of 3.7 ML is incorporated into the subsurface region (dashed curve). Again, the intensity of desorption peak β significantly decreases with increasing reaction temperature, whereas smaller intensity changes of peak α are observed. Moreover, the intensity of peak β continues to decrease even at higher reaction temperatures. After the reduction reaction with 1000 langmuirs of CO, the desorption spectra of both the smooth and the defect-rich surface are dominated by a larger peak α and a smaller peak β .

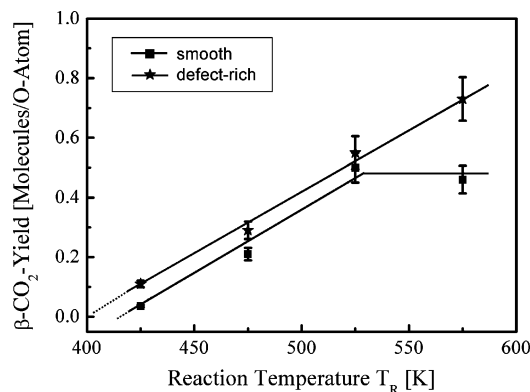


Figure 2. Comparison of the integral CO₂ yields at different T_R for the smooth and defect-rich surfaces derived from the intensity changes of desorption peak β of Figure 1a,b.

A rough estimate of the oxygen consumed during the reaction is obtained by deconvoluting the TD spectra with simple Gaussian distribution functions. Despite the apparent intensity change of peak α , this examination reveals that the amount of oxygen molecules desorbing via peak α corresponds to about 0.5 ML for both surfaces and all reaction conditions within the error bars. In other words, the intensity of peak α does not change with reaction temperature, the apparent change is solely caused by the broad shoulders of peak β . This result is in agreement with our previously published model for the oxygen desorption of non-oxidic states on Ru(0001).¹⁶ It assigns the emergence of peak α to the depletion of the subsurface reservoir until a minimum concentration of about 0.5 ML is reached. A low concentration of oxygen in the subsurface region leads to an increased binding energy of the chemisorbed oxygen on top of the first ruthenium layer, hampering the desorption of the remaining subsurface oxygen via the chemisorbed layer. This is reflected by the higher desorption temperature of peak α compared to peak β . Thus, the observed consumption of oxygen reacting to CO₂ stems from the β desorption peak only; therefore, the further analysis of the TD spectra will be limited to peak β .

With the knowledge of the initial (2.7 and 3.7 ML, respectively) and final oxygen coverage of the surface and the given CO exposure, it is possible to calculate the resulting CO₂ reaction yield using the number of impinging CO molecules ($\approx 10^{17} \text{ cm}^{-2} \text{ s}^{-1}$ for 1000 langmuirs) and the number of oxygen atoms consumed by the reaction. Figure 2 plots this CO₂ yield, due to desorption peak β , as a function of the reaction temperature. In general, both the defect-rich and the smooth surface exhibit the same trend of an increasing CO₂ yield with temperature. As one difference, the onset of the reaction is observed at $T_R \approx 425 \text{ K}$ for the smooth surface whereas the reaction already starts around 400 K for the defect-rich surface, demonstrating a dependence of the CO₂ yield on the defect density of the Ru(0001) surface. Obviously, already at temperatures of approximately 400 K subsurface oxygen atoms are mobile enough to diffuse to the surface. Here, they can replace oxygen atoms that have reacted with CO molecules before. This oxygen diffusion to the topmost ruthenium layer is enhanced if more defects are present. A second obvious difference between the two surfaces is the observation that the reaction yield seems to saturate at $T_R \geq 525 \text{ K}$ for the smooth surface whereas it continues to increase in the case of the defect-rich O/Ru surface. This behavior mirrors the depletion of subsurface oxygen, occurring earlier on the smooth surface due to the smaller initial oxygen coverage. When the minimum concentration of 0.5 ML

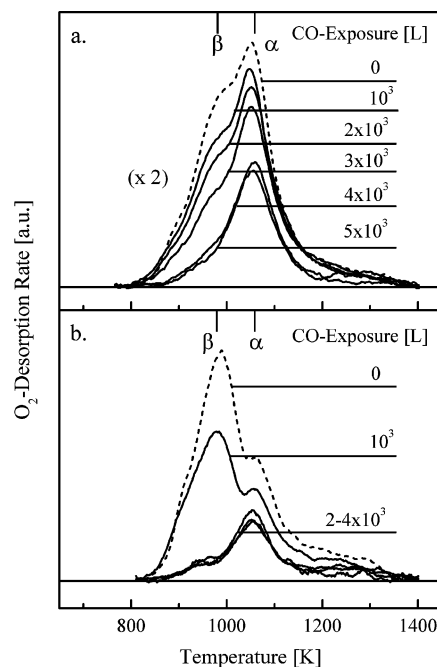


Figure 3. Comparison of the O₂ TDS before (dashed) and after the reaction (solid) of an oxidized smooth (a) and a defect-rich surface (b, $\rho = 0.4$) at $T_R = 475 \text{ K}$ with CO exposures of 1000–4000 langmuirs; the surfaces were oxidized with 10^{11} langmuirs of O₂ at $T_P = 475 \text{ K}$.

is reached, the bonds between the chemisorbed oxygen on top of the first ruthenium layer are strengthened and, under the given reaction conditions, the reaction comes to rest.

Because the oxidation reaction might be limited by the amount of CO exposure as well, experiments were performed with a fixed reaction temperature and different CO exposures. Figure 3 presents TD-spectra of a smooth and a defect-rich O/Ru surface containing 2.7 and 3.7 ML (top and bottom, respectively) before (dashed curves) and after CO exposure. To limit the exhaustion of subsurface oxygen for the smooth surface, the reactions were performed at a low sample temperature, $T_R = 475 \text{ K}$. On both surfaces, a pronounced decrease of the intensity of peak β with increasing CO exposure is observed. On the defect-rich surface, the desorption via peak β succumbs already for an exposure of 2000 langmuirs, indicating a nearly complete consumption of subsurface oxygen whereas on the smooth surface the oxygen desorption saturates only at 4000 langmuirs. The oxygen content remaining in the ruthenium crystal can be calculated by integrating the resulting TD spectra and calibrating them to a complete oxygen chemisorption layer, characterized by the broad desorption peak ranging from 1400 to 1040 K in Figures 1 and 3. The highest calculated oxygen consumption amounts to 2 and 1 ML for the defect-rich and the smooth surface, leaving approximately 0.7 ML oxygen in the subsurface region. The deconvolution process reveals a desorption of approximately 0.5 ML oxygen via peak α . Yet, after the reduction with 4000 langmuirs of CO, the desorption spectra of both the smooth and the defect-rich surface still exhibit a small contribution of peak β , slightly more visible in the spectrum of the defect-rich surface (Figure 3b). Because the oxygen incorporation can proceed also into deeper ruthenium layers,¹⁵ especially on a defect-rich surface, the remaining desorption at peak β is most likely correlated to oxygen atoms from deeper regions of the sample which could not contribute to the reaction under the given reaction conditions.

With the knowledge of the initial oxygen coverage (2.7 and 3.7 ML, respectively) and the given CO exposure, it is possible

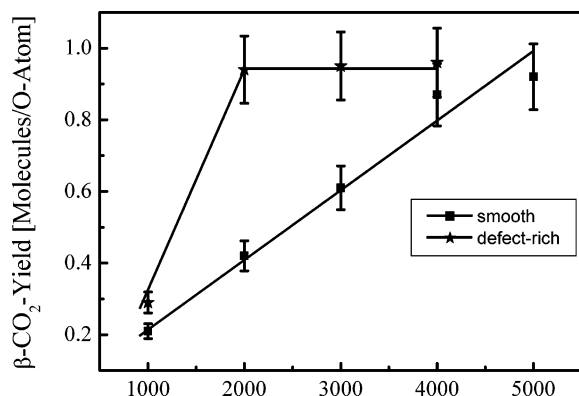


Figure 4. Comparison of the integral CO₂ yields for different CO exposures for the smooth and defect-rich surfaces derived from the intensity changes of desorption peak β in Figure 3a,b.

to calculate the CO₂ reaction yield resulting from peak β , depicted in Figure 4. For the defect-rich surface, the CO₂ yield reaches nearly 95% already for an exposure of 2000 langmuirs, indicating that virtually every oxygen atom is immediately reacting with an impinging CO molecule. To achieve a comparable yield on the smooth O/Ru surface, at least 5000 langmuirs of CO are required. This finding underlines the importance of defects for the reactivity of an oxygen-rich surface. First, their presence facilitates the oxygen incorporation into the subsurface region during preparation. Second, the CO oxidation process is assisted by the defect induced distortion of the crystal's structure leading to weakened O-Ru bonds on the ruthenium surface.

As an estimate for the reactivity of the oxide precursors, the integral CO/CO₂ conversion probability is calculated, given by the ratio of the number of oxygen atoms consumed during reaction and the number of impinging CO molecules ($\approx 3.1 \times 10^{17} \text{ cm}^{-2} \text{ s}^{-1}$ for 1000 langmuirs). For a defect-rich surface, this conversion probability yields 6×10^{-3} , which is 15 times the value observed for chemisorbed oxygen and comparable to the conversion probability observed for a Ru surface partly covered by bulk oxides (10^{-3} to 10^{-2}).¹⁰ This result is in good agreement with recent in situ XPS experiments under high-pressure conditions where a comparable activity of subsurface oxygen and oxide toward the CO oxidation was observed.²⁰

B. Changes of the Electronic Structure. Because the heating of the sample changes the state of the surface, monitoring the valence band region provides additional information about the binding state directly after the reaction. The upper panel in Figure 5 shows the spectra of a smooth (A) and a defect-rich (B, $\rho = 0.4$) Ru(0001) surface containing ≈ 2.7 and 3.7 ML of oxygen. The broad emission at $\approx 3.6 \text{ eV}$ (labeled peak IV), indicates large amounts of subsurface oxygen without the formation of oxide domains correlated to desorption peak β in TDS.^{16,18} After the exposure of both surfaces to 5000 langmuirs of CO at $T_R = 475 \text{ K}$ (C and D, respectively), the intensity of peak IV is decreased. Obviously, by replacing chemisorbed oxygen atoms on the surface that have been reacted-off with CO molecules, most of the subsurface oxygen has been consumed, in accordance with the results of the TDS measurements.

After the reaction, the UP spectra of the smooth (C) and defect-rich surface (D) exhibit three distinct peaks at 0.5, 2.3 and 5.8 eV (III, II, I). The same peak positions were found after the incorporation of 0.5 ML subsurface oxygen, correlated to desorption peak α in TDS, in clean smooth and defect-rich Ru(0001) surfaces at comparatively low oxygen exposures in

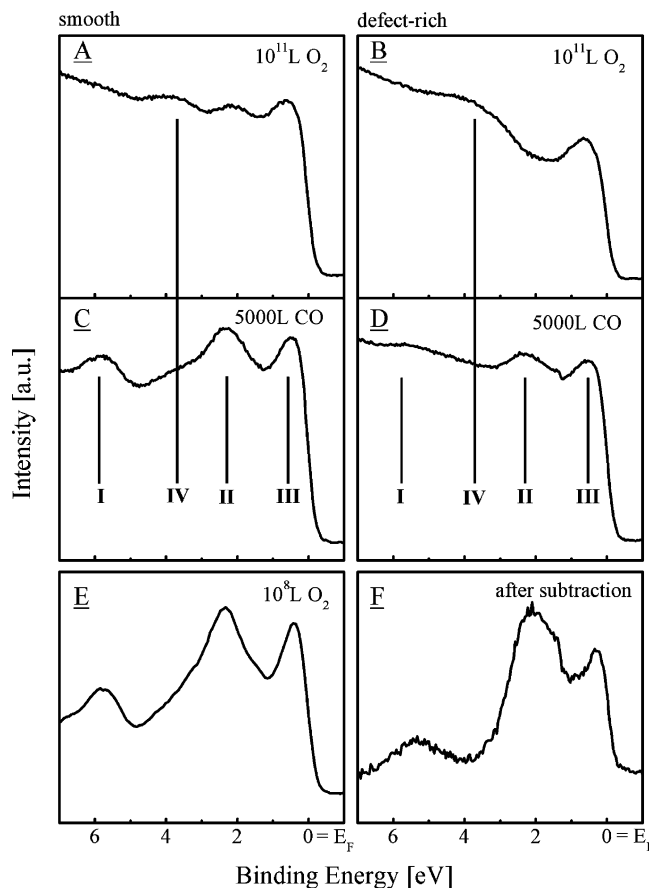


Figure 5. Comparison of UP spectra of an oxidized smooth and defect-rich Ru(0001) surface ($\rho = 0.4$) taken before (A and B, respectively) and after the reaction with 5000 langmuirs of CO at $T_R = 475 \text{ K}$ (C and D, respectively). The surfaces were oxidized with 10^{11} langmuirs of O₂ at $T_P = 475 \text{ K}$. Left: smooth surface. Right: defect-rich surface. Lower panel: (E) smooth surface oxidized with 10^8 langmuirs of O₂ at $T_P = 475 \text{ K}$; (F) spectrum obtained by subtraction of the spectrum of the freshly prepared (B) from the reduced defect-rich surface (D).

the LT regime. As an example, the spectrum of a smooth Ru(0001) surface exposed to 10^8 langmuirs at $T_P = 475 \text{ K}$ is depicted in Figure 5E. The peaks at 0.5, 2.3 and 5.8 eV are representative for oxygen atoms occupying the interlayer space beneath the smooth, not defected areas of the surface.¹⁸ Hence, a correlation of the spectra found after the reaction with a residual oxygen content of approximately 0.5 ML beneath the first ruthenium layer is plausible. Yet, one difference between the UP spectrum of a surface freshly prepared with subsurface oxygen and the spectra after the CO/CO₂ reaction is obvious: Compared to their “fresh” counterparts (e.g., spectrum E), the intensities of the peaks I–III appear weaker, both on the smooth and on the defect-rich surface (C and D, respectively). It was found that the sample temperature has a strong influence on the defect density of the surface, which decreases with increasing temperature.¹⁸ At the comparatively low-temperature $T_R = 475 \text{ K}$ oxygen in deeper regions of the bulk may be “trapped” by healing of defects located above and consequently be hindered to contribute to a reaction. Yet this oxygen may account for the weakening of the intensities of peak I–III by contributing to the background of the measured spectra.

To clarify this possible contribution of oxygen captured in deeper ruthenium layers, spectrum B of Figure 5 was used as a fingerprint for subsurface oxygen (represented by peak IV and desorption peak β in TDS, respectively) and subtracted from spectrum D in Figure 5. The resulting difference spectrum (F)

exhibits almost the same intensity ratios between peaks I, II, and III found for a freshly prepared surface with 0.5 ML assigned to oxygen atoms occupying the interlayer space beneath the first and second ruthenium layer. This finding hints to a small amount of subsurface oxygen remaining deeper in the bulk, which does not contribute to the reaction. Only by heating the sample to the desorption temperature do “buried” oxygen atoms become mobile enough to diffuse to the surface even without the presence of defects. This finding is in good agreement with the TD measurements of Figure 3 exhibiting a desorption not only at peak α but also at peak β , resulting in ≈ 0.7 ML of residual oxygen after the reaction with 4000 langmuirs of CO.

C. Reactive Molecular Beam Scattering. As described above, the reaction yield of the $\text{CO} + \text{O} \rightarrow \text{CO}_2$ reaction on O/Ru surfaces is controlled by the initial oxygen content, the CO exposure and the thermal activation. Another important aspect is the defect density with its strong influence on the overall reaction yield. In the following, we report on reactive molecular beam scattering experiments, shedding light on the possible reaction pathways, the reaction time scale and the dependence of the CO_2 yield on the defect density of oxide precursor covered surfaces.

As a first step, the change of the reaction yield with time was examined. A defect-rich ($\rho = 0.4$) and a smooth surface were prepared with 10^8 langmuirs of O_2 at $T_P = 550$ K (corresponding to 3 and 2 ML, respectively) forming oxide precursors in the vicinity of the surface.¹⁸ These surfaces were then exposed to a continuous CO beam with a flux of 3×10^{14} molecules/s. Figure 6 shows the temporal evolution of the CO_2 reaction yield on the smooth (a) and the defect-rich surface (b) for various reaction temperatures. At first sight, the temporal evolution of the reaction yield of both surfaces exhibits two different features accounting for two different reaction channels, similar to the results for oxidized surfaces.¹⁹ The reaction via the first “fast” path, labeled **1** in the following, starts as soon as the CO beams hits the surface and is already exhausted after approximately 15 s. This reaction can be observed even at $T_R = 385$ K. The CO_2 conversion yield via this fast reaction path increases up to temperatures of ≈ 500 K. Above a reaction temperature of 610 K the yield starts to decrease and nearly vanishes for $T_R = 660$ K, indicating a correlation with temperature induced changes of the sticking probability of CO.

At temperatures above $T_R \approx 430$ K a second contribution to the CO_2 yield can be observed, progressing on a longer time scale. Obviously, this reaction path is thermally activated. For both surfaces, the corresponding CO_2 yield reaches a maximum, with a higher yield for the defect-rich surface at $T_R \approx 610$ K (inset in Figure 6a: CO_2 yields of Figure 6a,b normalized to the CO_2 yield of a surface oxidized at 735 K). The maximum CO_2 yield at $T_R \approx 560$ K for the smooth surface is in good agreement with the temperature observed for the saturation of the CO_2 yield presented in Figure 2. At higher reaction temperatures the CO_2 yield decreases for both surfaces, reflecting the consumption of the subsurface oxygen reservoir.

The second contribution to the CO_2 yield is changing with time for higher T_R on the defect-rich surface (Figure 6b). In contrast, the reaction yield of the smooth surface exhibits a more uniform contribution to the CO_2 yield with time, changing with T_R only (Figure 6a). The observed differences in the time dependence of the reaction yield between a defect-rich and a smooth surface hint to two separate reaction channels. Both the time-dependent (dubbed **2** in the following) and the time-independent part of the reaction (named **3** in the following) are

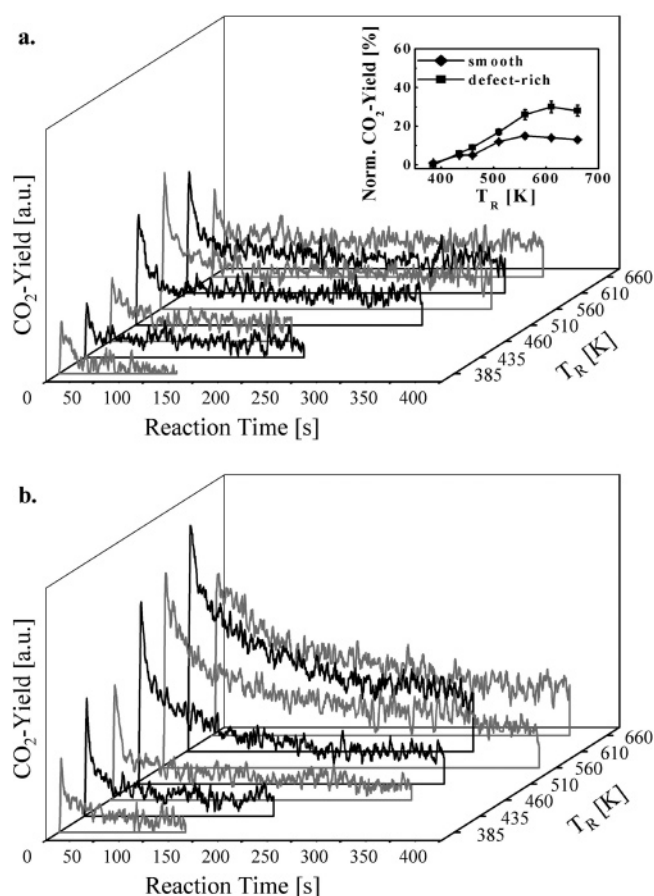


Figure 6. CO_2 yield of a smooth (a) and a defect-rich (b, $\rho = 0.4$) surface as a function of the exposure time for different reaction temperatures T_R between 385 and 660 K. Both Ru(0001) surfaces were oxidized with 10^8 langmuirs of O_2 at $T_P = 560$ K prior to reaction. Inset: integral CO_2 -yield of the smooth (\diamond) and the defect-rich (\blacksquare) Ru(0001) surface normalized to the CO_2 yield of a Ru(0001) surface oxidized at $T_P = 735$ K and 10^5 langmuirs.

thermally activated, contributing higher fractions to the reaction yield with increasing reaction temperature.

To distinguish the contributions of the suggested channels **2** and **3** to the overall CO/ CO_2 reaction yield, we prepared a nearly defect-free surface by modifying the standard treatment for sample cleaning.⁸ The preparation of such a surface (referred to as “extra smooth surface” in the following) was possible by repeatedly exposing a sputtered surface ($\rho = 0.4$) to high oxygen exposure (1 mbar) and subsequent annealing to 1550 K. The smaller defect density of the extra smooth surface compared to our “standard” smooth surface was verified by HAS. The nearly defect-free surface exhibits the linear decrease of the intensity of scattered helium atoms described by the Debye–Waller factor. The scattered helium intensity for the surface prepared according to the standard treatment is slightly smaller, but the same slope is observed. Only for temperatures above 1500 K is a small increase of the scattered helium intensity visible, reaching the intensity of the nearly defect-free surface at ≈ 1550 K.

Reactive scattering experiments with this extra smooth and a defect-rich ($\rho = 0.4$) surface containing the same amount of oxygen were performed at a fixed reaction temperature of $T_R = 560$ K. The integral oxygen content was varied between 1 and 3.7 ML for both surfaces. The influence of surface defects on the reaction can be directly seen in Figure 7, with both surfaces containing ≈ 2 ML of subsurface oxygen. For the extra

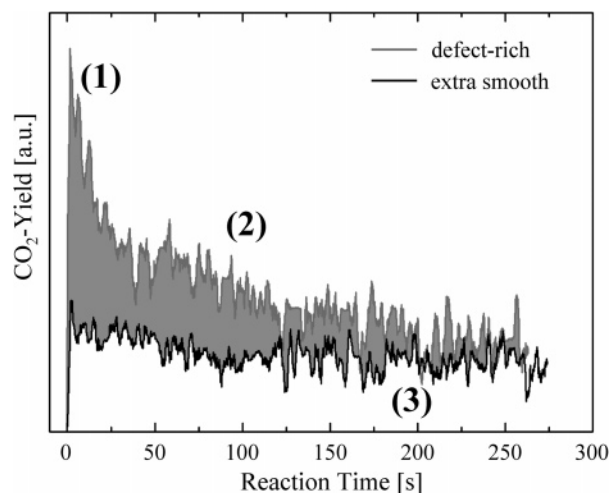


Figure 7. CO₂-yield of a defect-rich (gray line, $\rho = 0.4$) and a smooth (black line) surface each containing 3 ML of oxygen. Both surfaces were oxidized at $T_P = 500$ K. The numbers mark reaction channels 1–3, respectively.

smooth surface, the very fast reactions **1** and **2** are negligible, only the time-independent reaction path **3** can be observed. On the defect-rich surface the CO₂ yield of channel **1** ceases within ≈ 15 s whereas a further contribution of channel **2** is observed (both gray in Figure 7). After a total CO exposure time of approximately 170 s the CO₂ yields of the smooth and the defect-rich surface virtually exhibit no difference. The same behavior was observed for measurements with different oxygen contents of 1–3 ML. Hence, the difference in the reaction yield of the defect-rich and the smooth surface with increasing temperature (inset of Figure 6) can now be directly assigned to the fast (**1**) and the time-dependent reaction channels (**2**) with defect oxygen atoms as the active part in the reaction.

4. Discussion

The experimental results point to a correlation between the mechanisms responsible for the oxygen uptake directly beneath the topmost ruthenium layers and the reaction of oxygen with CO. Recently, it was shown that the formation of subsurface oxygen at $T_P \leq 550$ K can proceed either by diffusion of atomic oxygen via surface defects or by sinking of oxygen atoms chemisorbed in hcp or fcc sites through the first ruthenium layer and subsequent chemisorption of further oxygen.^{15,18,21} In addition, it was shown that subsequent annealing of a freshly prepared Ru(0001) sample loaded with subsurface oxygen to temperatures of ≈ 500 K practically does not change the amount of oxygen in the near-surface region as compared to a freshly prepared O/Ru surface.¹⁵ At this temperature, the subsurface oxygen atoms in the immediate vicinity of the surface are mobile enough to diffuse either through the topmost ruthenium layers to fill empty sites in the chemisorbed oxygen layer or to a defect site in the topmost ruthenium layer, thus contributing to a reaction. Hence, the temperature at which the CO oxidation reaction starts corresponds to the activation temperature for the oxygen incorporation into the subsurface region. This correspondence implies that the CO oxidation reaction can proceed by two different reaction sites, contributing to the observed intensity reduction of peak β in the TD spectra: (a) the reaction of CO at surface defects, accounting for a fast (**1**) and a time-dependent (**2**) path with oxygen adsorbed at or diffusing to a surface defect and (b) a time-independent reaction with chemisorbed oxygen in undisturbed surface areas (**3**).

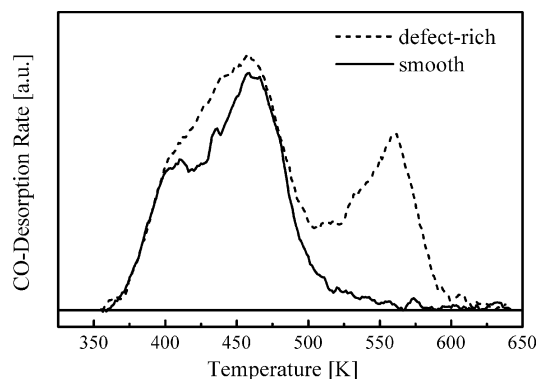


Figure 8. CO desorption spectra of a defect-rich (dashed line) and a smooth (solid line) Ru(0001) surface. The clean Ru(0001) surface was exposed to 5000 langmuirs of CO at room temperature.

On a defect-rich surface, reaction paths **1** and **2** through surface defects dominate. This is in agreement with the TD data (Figures 1 and 3), where a considerably higher CO₂ yield was observed for the defect-rich surfaces. Assuming a Langmuir–Hinshelwood (LH) mechanism, a CO molecule impinging from the gas phase needs to adsorb at the O/Ru surface. Because CO has a very short residence time on a Ru(0001) surface covered with a complete chemisorption layer, defects in the topmost layers of the ruthenium surface are required to provide vacant adsorption sites. Hence, a higher defect density of the surface increases the adsorption probability of CO molecules on ruthenium. This model is in agreement with both the TD data and the CO molecular beam scattering experiments. Thus, we assign reaction paths **1** and **2** to the Langmuir–Hinshelwood (LH) mechanism, which was considered the preferred reaction channel for surface defects on Ru(0001) also in theoretical studies.^{22,23}

The very fast reaction channel exhibits a strong CO₂ contribution within the first 15 s of reaction path **1**. From the experimental results, it is obvious that the corresponding CO₂ yield is not only limited in time but also limited by the reaction temperature. The maximum yield was observed for $T_R \approx 500$ K, diminishing rapidly at higher temperatures. Here, the residence time of CO molecules at defect sites becomes shorter. This is evidenced by TDS of CO desorbing from a clean Ru(0001) surface. The TDS exhibits a weaker peak at 410 K and an intense desorption feature at 460 K (Figure 8, solid line). Above 500 K the desorption rate is significantly reduced,^{24–26} accounting for the observed decrease of the contribution of reaction path **1** at $T_R > 500$ K. The time scale of the reaction suggests that only a limited number of oxygen atoms, probably adsorbed in the immediate vicinity of a defect site, is involved. Thus, following the LH mechanism, a temporarily adsorbed CO molecule can diffuse to a defect site and react with adjacent oxygen atoms. Because the oxygen available for this fast reaction channel is diffusion limited, oxygen atoms in close vicinity to defect sites on the surface are quickly depleted. For further reactions taking place, these sites have to be reoccupied. At $T_R \geq 430$ K and in the presence of structural defects, this can be achieved by subsurface oxygen diffusing to the surface and subsequently replacing the chemisorbed oxygen atoms already consumed in a prior reaction, leading to reaction path **2**. On a defect-rich surface, the probability for temporarily adsorbed CO molecules diffusing to defect sites and reacting with oxygen atoms is considerably higher than at a smooth surface. Finally, at a critical CO exposure of 2000 langmuirs virtually all oxygen atoms diffusing to the surface are instantly consumed

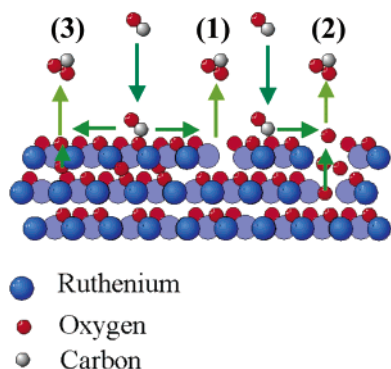


Figure 9. Model of the proposed reaction channels for the CO/CO₂ oxidation on Ru(0001). The numbers mark reaction channels 1–3, respectively.

by the reaction (see Figure 4). According to the CO-TDS, this process can proceed up to $T_R \approx 500$ K.

The proposed mechanism for reaction path 2 explains the observed maximum in the CO₂ yield on a smooth surface (Figure 2 and Inset Figure 6). Yet, for a smooth surface and, even more pronounced for a defect-rich surface, the reaction via path 2 continues at reaction temperatures above 500 K. This behavior can be understood by the examination of the CO desorption spectrum of a clean defect-rich surface (dashed line in Figure 8). Here, an additional desorption peak at 560 K is observed. Similar desorption features were reported for stepped Ru(109) and more open Ru(1120) surfaces and assigned to the recombination of dissociatively adsorbed CO on step edges.^{27,28} Thus, the dominance of reaction path 2 at higher reaction temperatures up to $T_R \approx 600$ K, in particular at a defect-rich surface, can be ascribed to the dissociative sticking of CO molecules. At reaction temperatures above 600 K, the CO₂ yield obtained via channel 2 is not increasing any further. This behavior can be explained by the reduced sticking probability of a CO molecule evidenced by the CO desorption data (Figure 8) and the diffusion rate of oxygen atoms to the defect sites limited by a given T_R . Even for high mobilities of diffusing oxygen atoms at elevated temperatures the consumption of subsurface oxygen is limited by the residence time of CO at the surface.

In the CO scattering data, another reaction path 3 is revealed. The CO₂ reaction yield of this path appears to be time-independent and is observed not only for the defect-rich but also for the extra smooth surface with reduced defect density. Thus, the mechanism responsible for the reaction cannot be correlated to structural defects. For a case without structural defects and vacancies in the chemisorption layer, theoretical studies predicted a direct reaction of impinging CO molecules with the chemisorbed oxygen as the most likely reaction path without prior adsorption of the CO.^{22,23} Under our experimental conditions, such an Eley–Rideal (ER) mechanism cannot be positively ruled out.

A factor accounting for the time-independent contribution of path 3 to the reaction yield is the oxygen diffusion to the surface. An oxygen atom filling an empty site at the surface has to diffuse through a densely packed ruthenium layer, a process that is most likely higher activated than the diffusion via a structural defect site, even for higher reaction temperatures. Thus, in this reaction path, CO molecules diffusing to and adsorbing at a vacancy in the chemisorption layer may even act as a promoter. This may allow subsurface oxygen atoms to segregate more easily to the surface, accounting for the higher

CO exposure needed to reach a CO₂ yield comparable to the defect-rich surface (see Figure 4). This suggestion is supported by recent in situ XPS experiments, which revealed pronounced intensity changes of the Ru 3d5/2 emission. There, the Ru 3d5/2 peak assigned to a complete chemisorbed oxygen layer exhibited a pronounced decrease during a reaction with CO.²⁰

Figure 9 provides a schematic overview of the proposed reaction pathways of the CO oxidation on O/Ru(0001).

Reaction paths 2 and 3 of the CO oxidation on Ru(0001) surfaces prepared under LT conditions strongly resemble the so-called Mars–Van Krevelen mechanism,²⁹ yet with subsurface oxygen atoms acting as a promoter of the reaction. This resemblance emphasizes the importance such oxide precursor states may play in more complex catalytic reactions.

5. Summary

The combination of reactive molecular beam scattering of CO and surface science techniques (TDS, UPS) provided new and detailed insights into the reaction mechanisms of the CO oxidation on oxide precursor states on Ru(0001). Under the reaction conditions investigated, three different reaction pathways could be identified. One is correlated to a fast reaction of oxygen with CO at defect sites. The other two are correlated to the reaction of subsurface oxygen diffusing via structural defect sites to the surface and to the reaction of chemisorbed oxygen. These latter reactions are thermally activated. The reaction yield was found to be higher on a defect-rich surface with an integral CO/CO₂ conversion probability of 6×10^{-3} in the case of a defect-rich O/Ru surface prepared at 475 K and an original oxygen content of ≈ 3.7 ML. This is a factor of 15 more than observed for chemisorbed oxygen and in the same order of magnitude as the conversion probability observed for a surface partly covered by bulk oxides (10^{-3} to 10^{-2}). This result is in good agreement with recent in situ XPS experiments under high-pressure conditions where a comparable activity toward the CO oxidation was observed.²⁰

Acknowledgment. R.B. and H.N. acknowledge the financial support by the DFG through project Ni-452. R.B. gratefully acknowledges the inspiring discussions with Robert Schlögl.

References and Notes

- (1) Driessen-Hölscher, B.; Niggemann, M. *J. Organomet. Chem.* **1998**, 570, 141.
- (2) Plietker, B.; Niggemann, M. *Org. Lett.* **2003**, 5, 3353.
- (3) Six, C.; Beck, K.; Wegner, A.; Leitner, W. *Organometallics* **2000**, 19, 4639.
- (4) Hoster, H.; Iwasita, T.; Baumgärtner, H.; Vielstich, W. *Phys. Chem. Chem. Phys.* **2001**, 3, 337.
- (5) Peden, C. H. F. *Surface Science of Catalysis: In Situ Probes and Reaction Kinetics*; American Chemical Society: Washington, DC, 1992.
- (6) Böttcher, A.; Niehus, H.; Schwegmann, S.; Over, H.; Ertl, G. *J. Phys. Chem. B* **1997**, 101, 11185.
- (7) Peden, C. H. F.; Goodman, D. W.; Wiesel, M. D.; Hoffmann, F. *M. Surf. Sci.* **1991**, 253, 44.
- (8) Maday, T. E.; Engelhardt, H. A.; Menzel, D. *Surf. Sci.* **1975**, 48, 304.
- (9) Böttcher, A.; Niehus, H. *J. Chem. Phys.* **1999**, 110, 3186.
- (10) Böttcher, A.; Niehus, H. *Phys. Stat. Sol. (A)* **1999**, 173, 101.
- (11) Kim, Y. D.; Over, H.; Krabbes, G.; Ertl, G. *Top. Catal.* **2001**, 14, 95.
- (12) Böttcher, A.; Krenzer, B.; Conrad, H.; Niehus, H. *Surf. Sci.* **2000**, 466, L811.
- (13) Böttcher, A.; Krenzer, B.; Conrad, H. *Surf. Sci.* **2002**, 504, 42.
- (14) Böttcher, A.; Starke, U.; Conrad, H.; Blume, R.; Niehus, H.; Gregoratti, L.; Kaulich, B.; Barinov, A.; Kiskinova, M. *J. Chem. Phys.* **2002**, 117, 8104.
- (15) Blume, R.; Niehus, H.; Conrad, H.; Böttcher, A.; Aballe, L.; Gregoratti, L.; Barinov, A.; Kiskinova, M. *J. Phys. Chem. B* **2005**, 109, 14052.

- (16) Blume, R.; Niehus, H.; Conrad, H.; Böttcher, A. *J. Chem. Phys.* **2004**, *120*, 3871.
- (17) Surnev, L.; Rangelov, G.; Bliznakov, G. *Surf. Sci.* **1985**, *159*, 299.
- (18) Blume, R.; Niehus, H.; Conrad, H.; Böttcher, A. *J. Phys. Chem. B* **2004**, *108*, 14332.
- (19) Böttcher, A.; Rogozia, M.; Niehus, H.; Over, H.; Ertl, G. *J. Phys. Chem. B* **1999**, *103*, 6267.
- (20) Blume, R.; Hävecker, M.; Zafeirotos, S.; Teschner, D.; Kleimenov, E.; Knop-Gericke, A.; Schlögl, R.; Barinov, A.; Dudin, P.; Kiskinova, M. *J. Catal.* **2006**, *239*, 354.
- (21) Todorova, M.; Li, W. X.; Ganduglia-Pirovano, M. V.; Stampfl, C.; Reuter, K.; Scheffler, M. *Phys. Rev. Lett.* **2002**, *89*, 96103.
- (22) Stampfl, C.; Scheffler, M. *Phys. Rev. Lett.* **1997**, *78*, 1500.
- (23) Stampfl, C.; Scheffler, M. *Surf. Sci.* **1997**, *377*, 808.
- (24) Buatier de Mongeot, F.; Scherer, M.; Gleich, B.; Kopatzki, E.; Behm, R. J. *Surf. Sci.* **1998**, *411*, 249.
- (25) Houle, F. A.; Hinsberg, W. D. *Surf. Sci.* **1995**, *338*, 329.
- (26) Pfnür, H.; Feulner, P.; Menzel, D. *J. Chem. Phys.* **1983**, *79*, 4613.
- (27) Zubkov, T.; Morgan, G. A., Jr.; Yates, J. T., Jr. *Chem. Phys. Lett.* **2002**, *362*, 181.
- (28) Wang, J.; Wang, Y.; Jacobi, K. *Surf. Sci.* **2001**, *488*, 83.
- (29) Centi, G. In *Catalysis from A to Z*; Cornils, B.; Hermann, W. A., Schlögl, R., Wang, C. H., Eds.; Wiley-VCH: Weinheim, 2000.